International Journal of Engineering, Management and Humanities (IJEMH)
Volume 5, Issue 3, May.-June, 2024 pp: 135-144 ISSN: 2584-2145
www.ijemh.com

The Effect of Annealing on the Structural, Optical and Electrical Properties of SnO_2Thin Film Prepared by Chemical Pyrolysis

Faraj Lakatan Kzar[1], Salim Oudah Mezan[1] Anwar Khairi Abed[2]
[1]*Republic of Iraq, Ministry of Education, Open Educational College, Studies Muthanna Centre.*
[2]*General Directorate of Education in Al-Muthanna Governorate, Ministry of Education, Iraq*

Date of Submission: 01-06-2024 Date of Acceptance: 10-06-2024

Abstract

SnO_2nonstructuralthin films were synthesized on the glass substrate usingchemical pyrolysis method in bath temperature 350 ˚C, byusing solution of $SnCl_2$ at 0.25M the films were annealed at (200, 400 and 450)˚C on annealed time of45 min.The structural propertieswere studied by using X – Ray Diffraction (XRD) also optical properties was studied from transmission spectrum, and the energy gap also was studied. The effect of annealing on grain size of film was determined by using AFM technique.

Keywords: Annealing, Structural, Optical, Electrical Properties, Thin Filme, Chemical Pyrolysis

I. Introduction

The investigation of SnO2 thin films has received a great amount of attention enough to their significant semiconducting properties, SnO2 is n-type semiconductor with considerable band gap(Eg > 3 eV). Thin films can be used as optoelectronic devices, photovoltaic cells, solar cell, chemical sensors, liquid crystal displays, photovoltaic cells, pellucid conducting electrodes, infrared reflectors, plasma display panels (PDPs) etc. [1-2]. etc. Semiconductor SnO_2-based gas sensors are widely reported in the literature [3-4].As well as, Tin oxide is useful as a hard film material for applications requiring high refractive and reflective properties. the fabrication of SnO_2 thin films on a solid substrate by the sputtering and the sol–gel process [5,6], Chemical vapor deposition [7], Sputtering [8,9], thermalevaporation [10], ultrasonic spray pyrolysis [11], ion-beam assisted deposition[12].

The resistivity of these films is found to depend on oxygen vacancies [13-15]. Annealing of the films can alter these characteristics apart from affecting the crystallinity and phases formed [16-19].This search aims toPreparation of membranes with the nonstructural by low-cost and easymethod and effectstudy and discuss the of particle size and annealing onstructural, optical properties and the mechanics of thin film response forgas sensor [20-22].

II. Experimental

The preparing of a solutionwas used for deposition membranes SnO_2, by usingchemical pyrolysis method in bath temperature 350˚C on the glass substrate.The material used was ($SnCl_2$: $2H_2O$) is a color white powder of concentration (0.25 M) and it dissolves (5.6gm) of the material in (200 ml) of a solution consisting of distilled water (60ml), methanol (45 ml) and hydrochloric acid center HCl (45 ml) and be gradual melting melt. The SnO_2 formulation can be represented as:

$SnCl_2 + 2H_2O \rightarrow SnO_2 + 2H_2\uparrow + Cl_2\uparrow$.

Film thickness was determined by a device(MINITEST – 3000) for measuring the thickness of the membrane 3.3 μm.

III. Results And Discussion

3-1 Structural properties

The Optical Transmitter Microscopic Examination:

In Figure (1: a, b, c and d)Shows the microscopic examination of the membranes of tin oxidebefore andannealing after annealing,notethedisappearanceofthe holes andthehomogeneitysurfaceandthe surfacebecomessofteraswellasthegranular borderdisappearance,when increasing of annealing temperature.The degree of disorder and defects present in the amorphous structure change due to heat treatment.

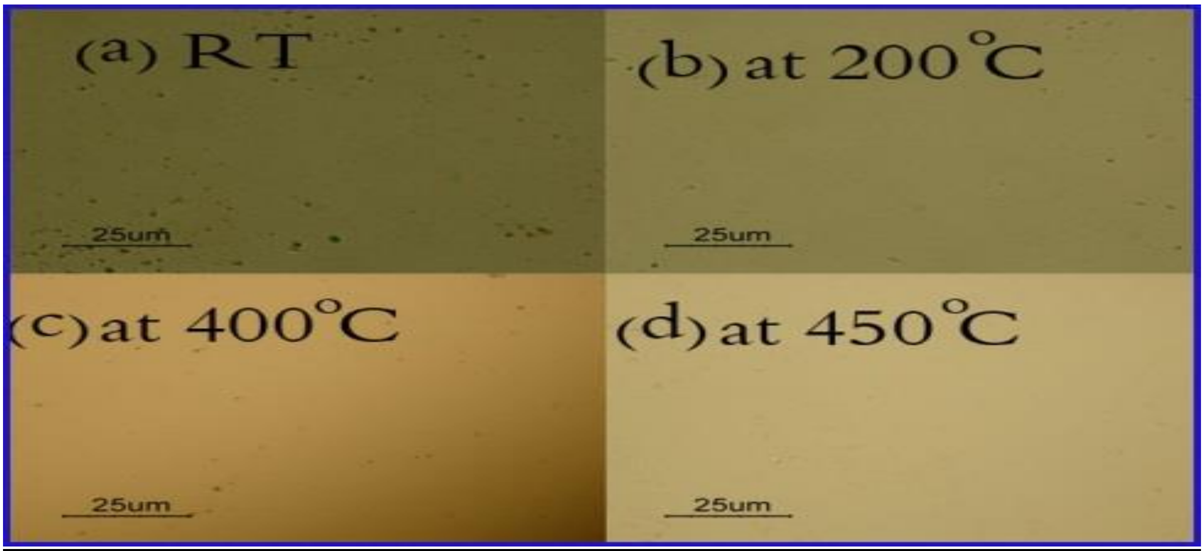

Fig(1).microscopic examination of SnO_2 thin film **(a)** as **-** deposited at RT. **(b)** annealing at 200˚C **(c)** annealing at 400˚C **and (d)** annealing at 450˚C

3.1 Atomic Force Microscopy (AFM)images:

AFM studies grains size in the as-deposited film before and after annealing as shown in the figure (2: a, b, c, and d). AFM images explain the grain size increase with increasing annealingtemperature. The annealing results in smoothening of the films lead to ordering of surface atoms to attain lower energy state.

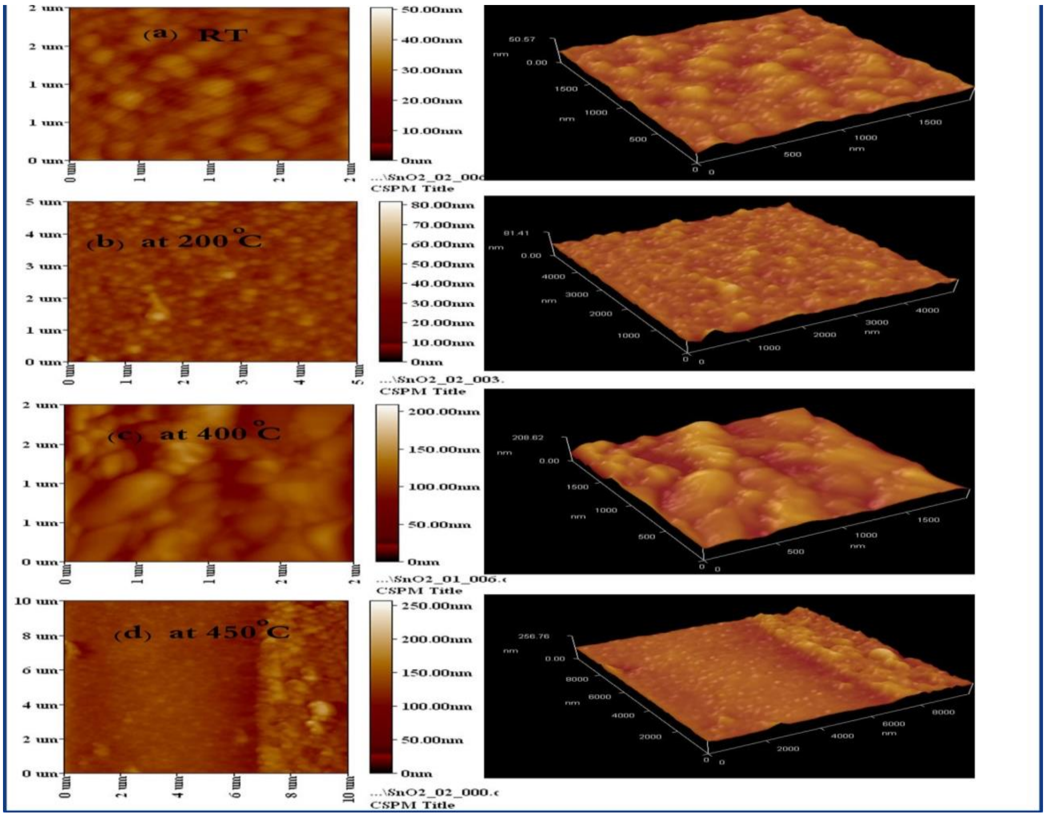

Fig. (2). AFM Images of SnO_2 thin film **(a)** as **-** deposited at RT. **(b)** annealing at 150˚C **(c)** annealing at 200˚C **and (d)** annealing at 450˚C

International Journal of Engineering, Management and Humanities (IJEMH)
Volume 5, Issue 3, May.-June, 2024 pp: 135-144 ISSN: 2584-2145
www.ijemh.com

3.2 X-Ray Diffraction(XRD)

The XRD studies was analyzed of thinfilm crystallinity as show figure(2 : a, b, cand d),TheXRD patterns of as-deposited , its amorphous structure as show figure (3:a) ,withannealedat 200^0 C ofSnO_2 films the figure(2: b)the reflection of (110),(200) and (211) as show in table 1, when annealedat 400^0 C and 450^0 C,note the emergence of a new phase (101)as show in table 2 and 3 , the figure(2:c and d) show that high temperature annealing has effect on the films deposited,the reflection from the (110), (101), (200) and (211) planes of SnO_2 for 2θ values of 26.55°, 33.83°, 37.92° and 51.77° respectively. These results comply with the standard SnO_2[XRD] X-ray diffraction data file [N 1997 JCPDS prevalent].

Grain size was calculated by compensation values that were obtained from the X-ray diffraction patterns of the previous figures in the Sherrer equation.

$D = K \lambda / \beta \cos\theta$

D: is the grain (G.S), K: is a constant (0.94), λ: is the wavelength of Cu Kα

θ: is the Bragg's angle and β : Full Width at Half Maximum (FWHM).

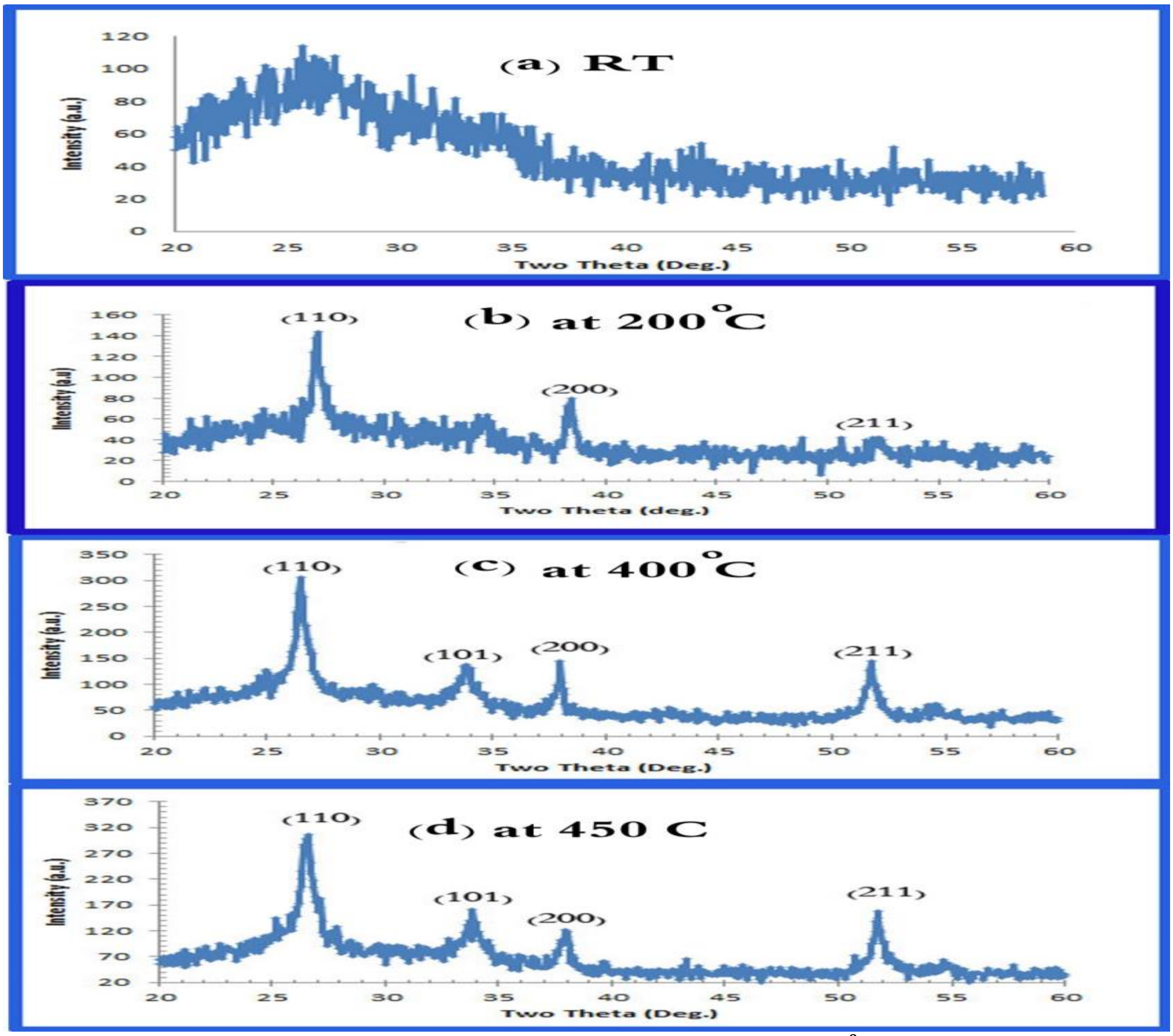

Fig. 3. XRD pattern of **(a)** as-deposited SnO_2 ; **(b)**annealing treated SnO_2(200)^0 C, 30 min.) ; **(c)** annealing treated SnO_2 (400)^0 C and **(d)**annealing treated SnO_2 (450)^0 C

Table .1: The properties of structure of SnO_2 film at annealing 200°C.

θ(deg.)2	d (A°)	I(a.u)	FWHM	hkl	G.s(nm)
26.64	3.77	100	0.74380	110	11.46
37.91	2.592	22	0. 52	200	16.87
51.87	1.68	18	0.65000	211	12.308

Table .2 : The properties of structure of SnO_2 film at annealing 400 °C.

θ(deg.)2	d (A°)	I(a.u)	FWHM	hkl	G.s(nm)
26.58	3.35	100	0.693	110	12.31
33.68	2.645	28	0.7432	101	11.66
37.94	2.372	54	0.491	200	17.86
51.57	1.765	42	0.610	211	15.13

Table .3: The properties of structure of SnO_2 film at annealing 450 °C.

θ(deg.)2	d (A°)	I(a.u)	FWHM	hkl	G.s(nm)
26.54	3.55	100	0.6740	110	12.47
33. 83	2.64	30	0.7400	101	11.72
37.92	2.37	59	0.4857	200	18.098
51.70	1.76	46	0.6014	211	15.34

3.3 Optical Properties: The optical properties were studied by measuring the transmission spectra in the wavelength range of 200-1200 nm by used Spectroscope to calculate the optical constants, absorption coefficient and optical band gap of the films. Figure (4: a, b, c and d) show the effect annealing on absorbance and transmittance at different temperature.Note when the annealing temperature increases the absorbancedecrease whiletransmittance increases. Theenergy gap decreases with the increase ofannealing temperatures of the SnO_2 films with, Since SnO_2 is an n-type semiconductor,as show in figure (5:a, b, c and d), alsonote that the value of absorption edge with annealing temperature change,as show in tables4 and 5.

International Journal of Engineering, Management and Humanities (IJEMH)
Volume 5, Issue 3, May.-June, 2024 pp: 135-144 ISSN: 2584-2145
www.ijemh.com

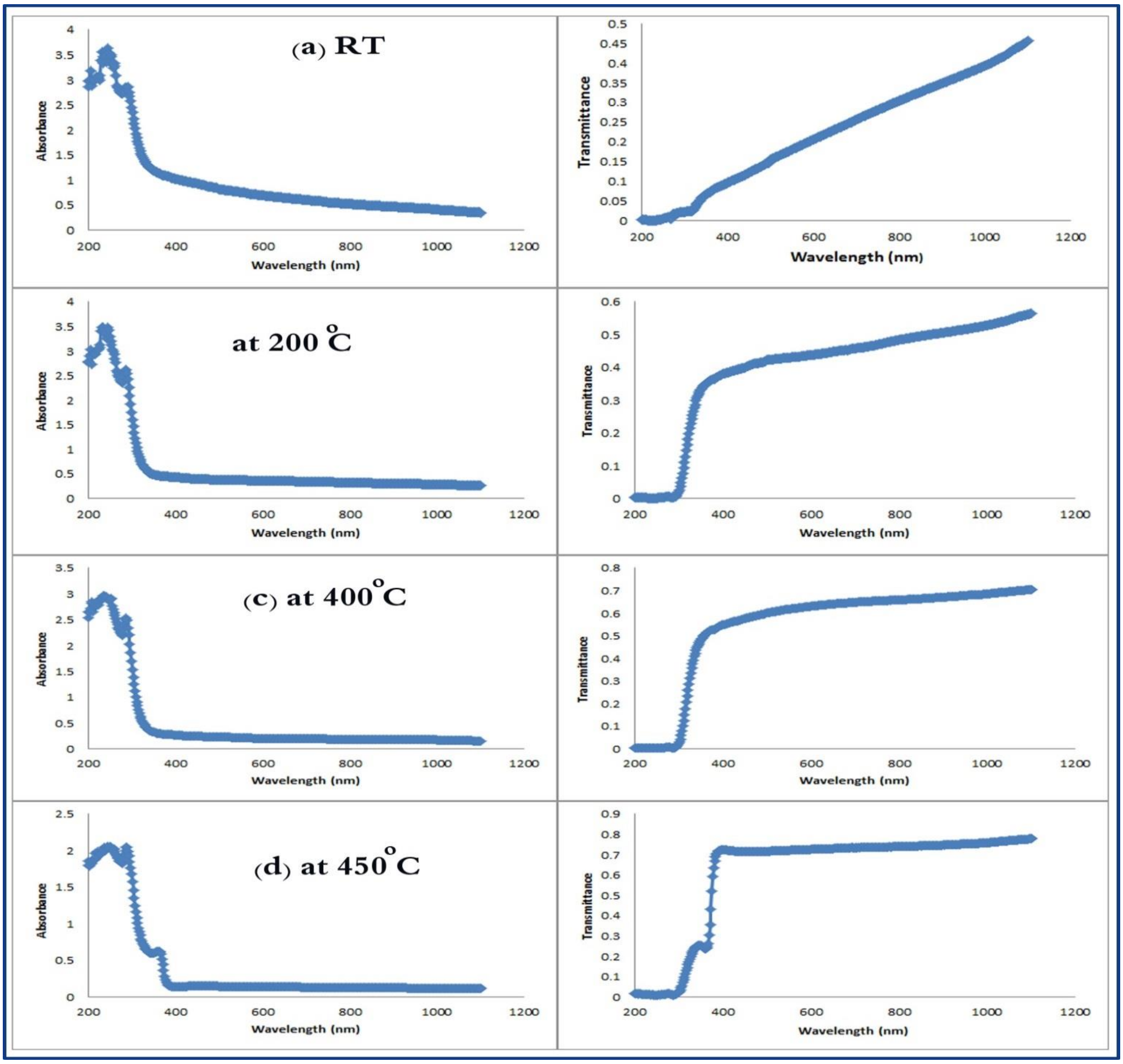

Figure 4. Optical transmission and absorbance spectra before and after annealing of SnO_2 films, (a) as-deposited SnO_2 (RT); (b) annealed at 200 ^{0} C; (c) annealed at 400 ^{0} C and (d) annealed at 450 ^{0} C

Energy gap (Eg) was determined by employing the following relation [18]

$\alpha = A(h\nu - Eg)^n / h\nu$

where α is absorption coefficient, A a constant (independent from ν) and n the exponent that depends upon the quantum selection rules for the particular material. The photon energy (hν) for y-axis can be calculated using Eq. (3).

$E = h\nu = hc/\lambda$

where h is Plank’s constant (6.626x10-34), c is speed of light (3x108) and λ is the wavelength.

International Journal of Engineering, Management and Humanities (IJEMH)
Volume 5, Issue 3, May.-June, 2024 pp: 135-144 ISSN: 2584-2145
www.ijemh.com

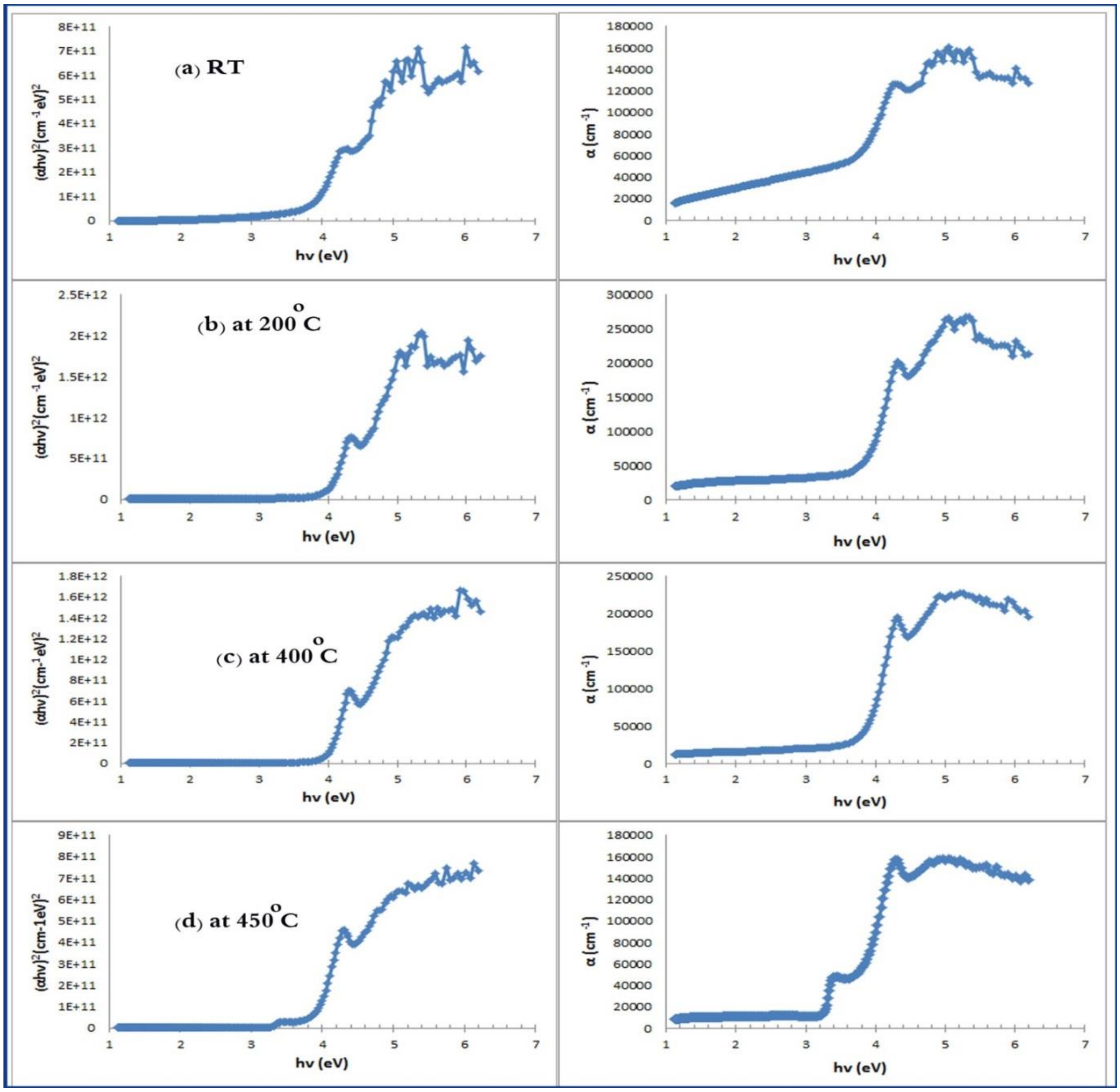

Figure 5.Energy gap and absorption coefficientspectra before and after annealing of SnO_2 films, (a) as-deposited SnO_2 (RT) ; (b) annealed at 200 ^{0} C; (c) annealed at 400 ^{0} C and (d) annealed at 450 ^{0} C

Table 4. Energy gap (Eg) values for tin oxide thin films(change the energy gap with before and after annealing).

SnO_2	**Eg (eV) Indirect**
(RT)	**4.02**
Annealed at 200ºC	**4.05**
Annealed at 400ºC	**4.01**
Annealed at 450ºC	**3.9**

Table 5. Absorption edge values for tin oxide thin films(change the absorption edge with before and after annealing).

SnO_2	**Absorption edge (eV)**
(RT)	**3.8**
Annealed at 200ºC	**3.75**
Annealed at 400ºC	**3.7**
Annealed at 450ºC	**3.65**

Table 6. The $\lambda_{cut\ off}$ values for tin oxide thin films(change the $\lambda_{cut\ off}$ with before and after annealing).

SnO_2	**λ_{cutoff}(nm)**
(RT)	**270**
Annealed at 200ºC	**265**
Annealed at 400ºC	**270**
Annealed at 450ºC	**265**

3.4 The Electrical Properties

3.4.1 Resistivity and Conductivity versus Temperature

The dc electrical conductivity, σ and resistivity,ρThe variation with 1000/T , as shown in Fig. 7were measured as a function of temperature.

The electrical conductivity (σ) can calculated by using following equations**:**

$\sigma = 1/\rho$

$\rho = R * wt/ L$

R :resistanceof thin film(ohm) ,**W:**widen thin film**(**cm**).** ,**t :** thin film thickness**(**cm**)** and

L :distance between aluminum electrodes

We can calculatethe description ofconductivity with temperature**.** Equation(6)

$\sigma = \sigma_\circ ex[E_a/K_B T]$

Where

$\sigma_\circ$:constant represent to conductivity at high temperature, Ea:electrical conductivity for activation energy, KB:Boltasmans constantand.T: Temperature

The electrical conductivity(σ) is found to decrease with increasing annealing temperatures.While resistivity(ρ) increases with increasing annealing. The electrical resistivity of SnO_2 thin films were studied at room te

se

fi

Figure 6.$\lambda_{\mathbf{cutoff}}$before and after annealing of SnO_2 films, (a) as-deposited SnO_2 (RT) ; (b) annealed at 200 ^{0} C; (c) annealed at 400 ^{0} C and (d) annealed at 450 ^{0} C.

International Journal of Engineering, Management and Humanities (IJEMH)
Volume 5, Issue 3, May.-June, 2024 pp: 135-144 ISSN: 2584-2145
www.ijemh.com

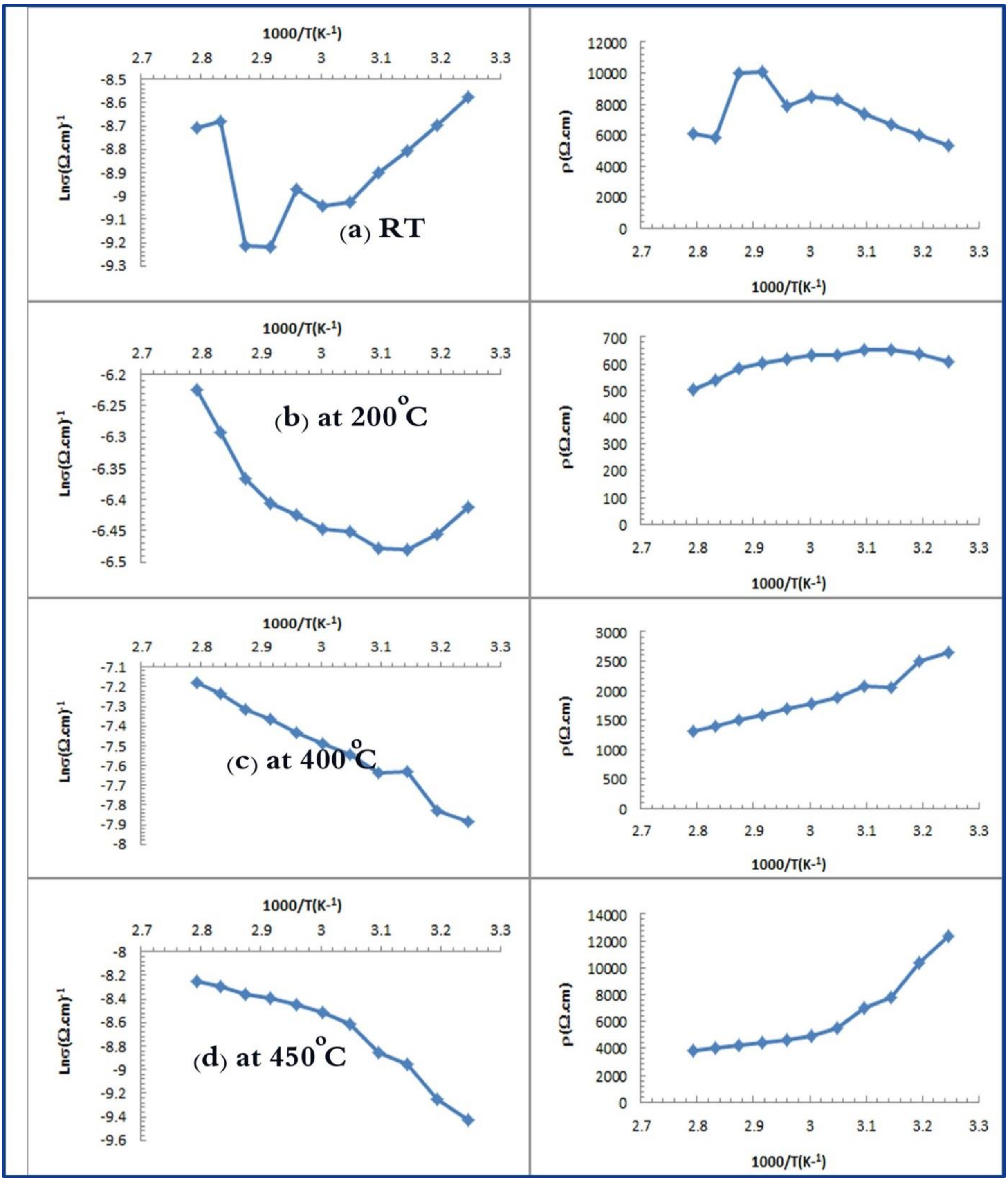

Figure 7.The variation of dc conductivity (σ_{dc}) and resistivity (ρ) with annealing temperature

2- The structural of $SnO_2$the film were done by X-Ray Diffraction (XRD) and AFM.

3- The films showed high transmittance with annealing temperaturesincreasing. While absorbance was decrease.Optical energy gap increase with increasing annealing temperatures.

IV. Conclusions

1- SnO_2 thin films prepared on glass substrate bychemical pyrolysis method in bath temperature 350˚C andannealing temperatures at 200ºC, 400ºC and 450ºC.

International Journal of Engineering, Management and Humanities (IJEMH)
Volume 5, Issue 3, May.-June, 2024 pp: 135-144 ISSN: 2584-2145
www.ijemh.com

4-The electrical conductivity increase with increasing annealing temperatures and electrical resistivity increase decreases with annealing temperatures increasing.

REFERENCES

[1]. W. Gopel, K. D. Schierbaum Sens. Actuators B **26** (1995)1. [2] R.S. Dale, C.S. Rastomjee, F.H. Potter, R.G. Egdell, Appl. Surf. Sci. **70/71** (1993) 359.

[2]. Mezan, S. O., Hello, K. M., Jabbar, A. H., Hamzah, M. Q., Tuama, A. N., Roslan, M. S., & Agam, M. A. (2020). Synthesis and Characterization of Enhanced Polyaniline Nanoparticles by Oxidizing Polymerization. Solid State Technology, 63(1), 256-266.

[3]. K. Hu, F. Wang, H. Liu, Y. Li, W. Zeng, Enhanced hydrogen gas sensing properties of Pd-doped SnO_2 nanofibres by Ar plasma treatment, Materials Science, Ceramics International, Volume 09, (2019), P.132.

[4]. K. Bunpanga,b, A. Wisitsoraatc,d,e, A. Tuantranontc,e, S. Singkammof, S. Phanichphantc, C.Liewhirana,c,g, Highly selective and sensitive CH_4 gas sensors - spray-made Cr-doped SnO_2 Sensors and Actuators B: Chemical, Volume 291, 2019, p.p177-191

[5]. Turki Jalil, A., Emad Al Qurabiy, H., Hussain Dilfy, S., Oudah Meza, S., Aravindhan, S., M Kadhim, M., & M Aljeboree, A. (2021). CuO/ZrO_2 nanocomposites: facile synthesis, characterization and photocatalytic degradation of tetracycline antibiotic. *Journal of Nanostructures*, *11*(2), 333-346.

[6]. T. Minami, H. Nanto, S. Takata, Jpn. J. Appl. Phys. 23 _1984. L280.

[7]. K. Hu, F. Wang, H. Liu, Y. Li, W. Zeng, Enhanced hydrogen gas sensing properties of Pd-doped SnO_2 nanofibres by Ar plasma treatment, Materials Science, Ceramics International, Volume09, (2019), P.132

[8]. Mezan, S. O. (2023). Enhancing the Morphological and Physical Characteristics of Zinc Sulphide Thin Films for Solar Cell Use during Manufacturing.

[9]. Saleh, R. O., Mansouri, S., Hammoud, A., Rodrigues, P., Mezan, S. O., Deorari, M., & Shakir, M. N. (2023). Dual-mode colorimetric and fluorescence biosensors for the detection of foodborne bacteria. Clinica Chimica Acta, 117741.

[10]. Tesleva, E., Akhmetov, L. G., Zalilov, R., Kadhim, M. M., & Jalil, A. T. Application of Vortex Generators to Remove Heat Trapped in Closed Channels.

[11]. S.P. Choudhurya*, S.D. Gunjalb,c, N. Kumarid, K.D. Diwatee, K.C. Mohiteb, A. Bhattacharjeea Facile synthesis of SnO_2 thin film by spray pyrolysis technique and investigation of the structural,optical and electrical properties , materialstoday,Volum 3, Issue 6, (2016),P.P 1609-1619

[12]. Vossen J L and Poliniak E S 1972 *Thin Solid Films* **13** 281

[13]. C.N. Xu, J. Tamaki, N. Miura, N. Yamazoe, Grain size effects on gas sensitivity of porous SnO_2-based elements, Sens. Actuators B 3 (1991) 147.

[14]. A.O.-Flores, P.B.-Perez, R.C.-Rodriguez, A.I. Oliva, Rev. Mex. Fis. **52** (2006) 15.

[15]. Tesleva, E., Akhmetov, L. G., Zalilov, R., Kadhim, M. M., & Jalil, A. T. Application of Vortex Generators to Remove Heat Trapped in Closed Channels.

[16]. Oudah Mezan, S., & Khalaf Jabbar, K. (2024). Green synthesis of copper (II) oxide nanoparticles using lemon leaves and optimization for characterization. *Journal of Nanostructures*.

[17]. M. Suzuki, H. Ohdaira,T. Matsumi, T. Matsumi, T.kumeda,T. Shimizu, T. J. Appl. Phys. 16, 221 (1977).

[18]. Hasan Jabbar, A., Oudah Mezan, S., Alameri, A. A., Prakaash, A. S., Mohammed Baqir Al-Dhalimy, A., & Younes, A. (2024). Fe_3O_4@ Diamine-CuI Nanocomposite: A Novel and Highly Reusable Nanomagnetic Catalyst for Ecofriendly Synthesis of Triaryl Imidazoles. *Polycyclic Aromatic Compounds*, *44*(2), 1309-1325.

[19]. Maseer, M. M., Alnaimi, F. B. I., Hannun, R. M., Wai, L. C., Al-Gburi, K. A. H., & Mezan, S. O. (2022). A review of the characters of nanofluids used in the cooling of a photovoltaic-thermal collector. Materials Today: Proceedings, 57, 329-336.

[20]. Mansouri, S., Mezan, S. O., Altalbawy, F. M., Kareem, A. K., Alhachami, F. R., Ramírez-Coronel, A. A., ... & Jawhar, Z. H. (2023). Recent advances in assembly strategies of new advanced materials-based analytical methods for the detection of

cardiac biomarkers as a diagnosis tool. Microchemical Journal, 108827.

[21]. Mezan, S. O. (2023). Synthesis and characterization of laser irradiated polyaniline/rice husk (silica) nanocomposites for electrical conductivity applications (Doctoral dissertation, Universiti Tun Hussein Onn Malaysia).

[22]. Al-Hakeim, H. K., Abed, A. K., Almulla, A. F., Moustafa, S. R., & Maes, M. (2023). Anxiety due to Long COVID is partially driven by activation of the tryptophan catabolite (TRYCAT) pathway. Asian Journal of Psychiatry, 88, 103723.